Nomograms in the history and education of machine mechanics*

Giovanni Mottola [1*] and Marco Cocconcelli [1]

[1]Department of Sciences and Methods for Engineering, University of Modena and Reggio Emilia, Via G. Amendola 2, Reggio Emilia, 42122, Italy.

*Corresponding author. E-mail: giovanni.mottola@unimore.it

Abstract

Computing formulae and solving equations are essential elements of scientific analysis. While today digital tools are almost always applied, analog computing is a rich part of the larger history of science and technology. Graphical methods are an integral element of computing history and still find some use today. This paper presents the history of nomograms, a historically-relevant tool for solving mathematical problems in various branches of science and engineering; in particular, we consider their role in mechanical engineering, especially for education, and discuss their mathematical properties. Each nomogram is a graphical description of a specific mathematical equation, designed such that the solution can be found through a simple geometric construction that can be performed with a straightedge. By design, using nomograms requires little skills and can be done even in adverse environments; a solution of sufficient accuracy for most purposes can then be found in a very short time. Another important advantage of nomograms is that they offer clear insight on the relationships between the variables, an insight which can be lost by looking at a complex equation. First introduced in the late 19th century, nomograms were used by engineers and scientists due to their speed with respect to manual calculations, before being superseded by computers. While now mostly obsolete in practice, nomograms can still prove useful in workshops and teaching classes: we thus also discuss their educational applications and present a few original examples.

Keywords: nomograms, history of machines and mechanisms, mechanical engineering education, graphical computing, mechanics of machines

*This paper is an extended version of our work *"Nomograms: an old tool with new applications"* presented at the *"7th International Symposium on History of Machines and Mechanisms (HMM 2021)"*, Jaén, Spain, 28–30 April 2022.

1 Introduction

In science and engineering, the analysis of a specific problem frequently leads to a physical model, which in turn provides one or more mathematical equations to be solved. Commonly, these equations correlate several scalar parameters, so that a subset of them can be derived as functions of the other ones: consider, for instance, the parameters for the design of a mechanical component with respect to the input constraints. We are interested in equations that have a finite number of solutions, which can then be computed; in other words, we disregard equations which define a multi-dimensional boundary (with infinitely many points).

For all but the simplest equations found in practice, the solution process requires some computational device, as the mathematical steps are usually tedious (or even prohibitively long) to perform by hand. In fact, large research centers such as NASA used to hire teams of human computers, who were assigned a list of arithmetical operations to be performed (Grier, 2001). Hand calculations, however, have a high risk of errors, where all the results after a single mistake may be invalid: this is due also to the lack of insight over the intermediate results, which are often difficult to check.

An alternative once in common use are *graphical methods*, some of which have been known since antiquity. These methods are defined by the tools used, such as writing devices, straightedges and compasses: the mathematical problem is then turned into an equivalent geometrical problem, which is solved by a corresponding construction. Due to their design, graphical methods can be much faster than analytical procedures; moreover, they are generally more intuitive to understand, even for users with limited mathematical proficiency. Finally, the visualization of the data is intrinsic in the solution process: this makes it easier to spot potential errors, but also provides insight over the relationships between the parameters. On the other hand, graphical methods have fixed accuracy (due to the tools used and to the manual dexterity of the user), which is however more than sufficient in most cases.

For the advantages outlined above, graphical methods used to be (and, in part, still are) commonly used by researchers, particularly in engineering education and practice, where larger approximations are acceptable. However, they have now been largely surpassed by digital methods: the advent of personal computers in the latter half of the 20$^{\text{th}}$ century made large-scale computations affordable and immediate and general-purpose software for equation solving is now a default tool for these problems. Nevertheless, graphical methods are still worth studying, if nothing else as part of the broader history of science and as teaching tools to introduce complex concepts.

Among other graphical tools, *nomograms* (d'Ocagne, 1899) are systems of *scales* (that is, parametric curves in one variable), designed in such a way that the mathematical relationship between the variables can be equivalently expressed in a simple geometric form, such as the collinearity of three points. Therefore, a nomogram can be used to solve an equation by choosing the variables that are designed as inputs and marking the corresponding point on the respective scales; the solution is then found by a geometrical construction which can be performed by tools such as a straightedge[1]. Due to their advantages, nomograms used to be a staple of engineering practice, together with

[1]Sometimes, thin threads of wire may be used to mark lines, to allow reusing the nomogram after each calculation.

devices such as slide rules. We are especially interested in their role within the field of mechanical engineering, a role that we will discuss through our bibliographic research.

While no longer common today, nomography still has its applications, for instance where digital tools such as spreadsheets would be inconvenient: considering for instance shop-floor operations and open-field research, printed nomograms appear interesting due to their ruggedness and portability. Moreover, nomography can be used as a teaching tool, which helps to explain complex topics through a clear visualization.

In this paper, we aim to present the history of nomography from an engineers' perspective, in particular within the field of Mechanisms and Machine Science. We thus discuss the development of nomograms and their historical precursors, together with the mathematical research on the properties of nomograms. We also present a few original examples that we created to show possible applications of nomograms for educational purposes and to discuss guidelines in the development of such tools. We believe that similar examples can be useful both for inspiring interest among engineering students towards the history of our discipline and to elucidate mathematical concepts that would be otherwise difficult to visualize. In our work, we used the open-source nomographic library *pyNomo* (Boulet et al., 2020), developed in the Python programming language, to create visually attractive graphs (as high-quality vector images) in an automated way that is much quicker than traditional manual approaches.

The remainder of this paper is structured as follows. In Sec. 2, we discuss the history of nomography, with a focus on their application in mechanical design. We then present the mathematical properties of nomograms and the methods to design new ones in Sec. 3; we also discuss how simple nomograms can be combined to solve equations of several variables. Later, in Sec. 4, we present selected nomograms and their potential industrial and educational applications; these nomograms are original (to the best of our knowledge) and useful to understand the advantages and limitations of these tools. Finally, we offer our conclusions and directions for future work in Sec. 5.

2 Nomograms in history

For more than a century, nomograms were researched by mathematicians and taught in technical education programs. Due to their past significance, nomograms were analyzed in terms of their historical development in several review works, such as (Doerfler, 2009; Evesham, 1986, 2010; Hankins, 1999; Tournès, 2003); however, to the best of our knowledge, no such reviews have been presented from the perspective of engineers.

To define the scope of our research, we only consider purely graphic approaches that require nothing more than pencil and straightedge. Thus, we disregard approaches that use complex mobile elements: for instance, we will not discuss the role of *slide rules*, another instrument (conceptually related to nomograms) that was in use until the '60s.

We remark that the terminology is not unequivocal: several works on "nomograms" use in fact graphical methods that are quite different—and generally more cumbersome to use—than standard nomograms (Grimes, 2008), such as graphs having one or more lookup curves with data from experiments or previous calculations. Here, instead, we only consider methods that require some geometrical construction. Moreover, especially in older sources, alternative terms such as "nomographs", "alignment charts"

and "abacs" are used interchangeably (Doerfler, 2009). To avoid confusion, in this paper we always use the term "nomogram", first introduced by French mathematician and engineer Maurice d'Ocagne (1862–1938) in the late 19th century (d'Ocagne, 1899) to distinguish his work from previous contributions: our bibliographic search on scholarly research engines shows that this expression remains the prevalent one.

2.1 Invention and diffusion: 1800–1960

In the history of mathematics, nomogram (from the Greek words νόμος, meaning "law", and γραμμή, meaning "line") is a relatively recent term, which should not be applied to computing tools introduced before the seminal work by d'Ocagne (Evesham, 1986); at the same time, d'Ocagne was influenced in his ideas by several other authors, from whose we can understand the main concepts of nomography as he developed it.

Several mechanical devices have been developed since antiquity to ease complex computations; in most examples, the user keeps track of numbers and of their respective relationships by using movable components. An example is the *abacus*, using beads moving on wires. Devices that can be identified as precursors to nomograms include:

1. Astronomical instruments (Evesham, 1986; Tournès, 2003), such as *astrolabes* and *equatoria*, used to compute the position of the Sun, the Moon and the planets; examples are the *Albion* by Richard of Wallingford (early 1300s) and the *jovilabe* (1600s) used by Galileo Galilei to study the orbits of the moons of Jupiter.
2. *Sundials* (Evesham, 1986; Glasser & Doerfler, 2019) and *moondials* (Tournès, 2003); while strictly speaking these are not computing instruments, they are nevertheless based on calculations and present graphically their results.
3. *Volvelles* and *slide charts* (Evesham, 1986), which are closely related to the slide rules mentioned earlier; these tools are composed of movable pieces of paper and, as for nomograms, each of them is designed for a specific computation.

The first essential tool for d'Ocagne's work was *coordinate geometry*, developed in the 17th century by French mathematician René Descartes (1596–1650); having defined a coordinate system, we can draw the graph of a function F. In the following, we consider mostly nomograms in three variables, providing solutions to the equation

$$F(v_1, v_2, v_3) = 0 \tag{1}$$

We define auxiliary functions F_i, each depending on the variables of interest v_i and on the coordinates x and y on a Cartesian plane: the F_i's are such that the set of equations

$$\begin{cases} F_1(x, y, v_1) = 0 \\ F_2(x, y, v_2) = 0 \\ F_3(x, y, v_3) = 0 \end{cases} \tag{2}$$

holds if and only if Eq. (1) is satisfied. Then, three parametric families of curves in the x-y plane can be graphed, one for each of the equations in (2). In each family, a specific curve corresponds to the set of points that satisfy the defining equation, for a fixed value of the variable v_i; each family can then also be seen as the set of level curves for

the corresponding equation. A point at the intersection of three curves (one for each family) is then a solution to Eq. (1). Clearly, the problem of expressing Eq. (1) in the form (2) is *undetermined*, as there are in general infinitely many possible choices for the equivalent system of equations; the choice of the functions F_i in (2) is then guided by convenience or mathematical insight. In a practical case, no exact intersection of three curves is found, as the sets of level curves must be discretized (to avoid cluttering the graph); the curves corresponding to the values of the input variables (which may be any two of the v_i's) closest to the ones for the problem at hand are then selected and the final result is found from simple graphical interpolation. Some of the main features of nomograms can already be recognized in this simpler concept, as follows.

- From two values v_i, the third can be derived graphically, even if the relationship in Eq. (1) cannot be inverted analytically; solving *direct* and *inverse* problems (depending on which variables are defined as input) is thus equivalently easy.
- The *approximation* of a given solution is related to its distance from the closest curve of the output variable, thus providing a visual feedback of the error.
- The *precision* is limited by the resolution of the graph and by the user's skills, especially in approximating a quasi-exact solution; however, large errors due to misreading are unlikely, and out-of-scale errors are outright impossible, since only the curves corresponding to meaningful ranges for the v_i's are plotted.
- Each graph is targeted for a *specific* equation, while other calculating devices (such as slide rules) are more general; however, the method presented above is *general* and a graph can be devised for almost any equation found in practice.

In Eq. (2), one may take, for simplicity, $F_1 = v_1 - x$ and $F_2 = v_2 - y$; then, we can set $F_3 = F$. The nomogram is then obtained by drawing on the x-y plane the level curves (called *isopleths*) corresponding to constant values of F. An example of the resulting graph is shown in Fig. 1a, for the case $F = v_3 - v_2 v_1 = 0$; with this graph, one may then find the product v_3 of two variables v_1 and v_2. This is in fact the first known application of this concept (also called an *intersection nomogram*), originally presented by French manufacturer Louis-Ézéchiel Pouchet (1748–1809): this way, he generalized the *discrete* multiplication tables (known since Pythagoras) as *continuous* curves, namely hyperbolas. Multiplying non-integer numbers is also possible through interpolation. Pouchet's work is also historically significant as he was the first to introduce the expression "graphical calculus" to describe his approach (Tournès, 2000).

One issue of the method above is that it requires graphing complex curves on paper, which in Pouchet's time was a time-consuming task done by hand. A first improvement was offered by French engineer Léon-Louis Lalanne (1811–1892), who suggested to use *nonlinear* scales for graphs. Consider again the multiplication graph introduced by Pouchet: the isopleths in this case are given by $v_1 v_2 = C$, with C being a constant value. If the values of v_1 and v_2 are reported on logarithmic axes, however, the graph can be simplified: indeed, taking the logarithm of both sides in the equation $v_1 v_2 = C$, one has $\log(v_1) + \log(v_2) = \log(C)$, meaning that on a log-log plot the isopleths become straight lines. While drawing nonlinear scales is somewhat more complex, the advantage of drawing straight lines (instead of curves) more than compensates this drawback, since straight lines, which are defined by two points, are much easier to

plot. As an example, the graph in Fig. 1a has been redrawn in Fig. 1b using nonlinear scales for the v_i's. Lalanne called his concept *anamorphosis*, a painting technique using deliberately exaggerated projective distortions. The use of nonlinear scales later became an essential tool in devising simple nomograms for complex equations.

The final elements in this development were progressively introduced by d'Ocagne in several works on graphical calculus in the late 1800s; this research finally culminated in the first book (d'Ocagne, 1899) on nomography proper. There, the author put to use the tools of *projective geometry*, a branch that had recently been introduced by French engineer and mathematician Jean-Victor Poncelet (1788–1867) and others. In particular, through the principle of *duality* between points and lines, d'Ocagne represented each straight line in an anamorphic graph by a single point; then, the condition of having three curves through a common point corresponds to having three points aligned on the same line. This also simplifies the reading of the nomogram, which is much less cluttered: one only needs to draw a straight line through two points, whose positions are defined by the two input variables, to find the third point, which provides the output value. The other idea advanced by d'Ocagne was to substitute the (orthogonal) coordinate axes with three curves C_i $(i = 1, 2, 3)$ in the plane, thus introducing *alignment nomograms*. Each variable v_i then defines a point P_i on the corresponding curve, which is graded along its length; the scale may be linear or nonlinear (Fig. 1c and 1d), depending on which approach makes the resulting nomogram simpler to draw and to use. Each curve is defined parametrically as $C_i(v_i) = \big(f_{ix}(v_i), f_{iy}(v_i)\big)$ in the Cartesian plane; the condition for alignment of three points is then given by

$$\begin{vmatrix} f_{1x}(v_1) & f_{1y}(v_1) & 1 \\ f_{2x}(v_2) & f_{2y}(v_2) & 1 \\ f_{3x}(v_3) & f_{3y}(v_3) & 1 \end{vmatrix} = 0 \tag{3}$$

(notice that the determinant in Eq. (3) is equal to the area of triangle $\triangle P_1P_2P_3$, which is zero if the points P_i are aligned). If a function $F(v_1, v_2, v_3)$ can be rewritten in the form shown in Eq. (3), then a nomogram can be developed for solving Eq. (1).

An advantage of alignment nomograms is that they allow us to easily solve equations in more than three variables; for instance, to solve $F(v_1, v_2, v_3, v_4, v_5) = 0$, one may first derive v_3 from v_1 and v_2, and then find v_5 from the v_3 thus obtained and v_4. The two corresponding nomograms (for the two steps of the solution) can then be combined, by having a curve C_3 that is common to both. While writing an equation in this form is a complex problem in general (and is unsolvable in some cases), the resulting nomogram is significantly easier to use and understand than an intersection nomogram. In this case, as for intersection nomograms, the graphical representation of a given equation is not unique: with a different choice of scaling (such as logarithmic scales instead of linear) the nomogram is defined by different curves. One can also modify a nomogram by multiplying the matrix in Eq. (3) by another constant matrix, and then taking the determinant: geometrically, this is equivalent to a linear transformation in the plane (such as scaling, rotating, translating, stretching or shearing) and it results in another nomogram that may be easier to read (but still solves the original equation). Creating easy-to-use nomograms thus required skill and experience in d'Ocagne's time, a limitation that can now be overcome through software (Boulet et al., 2020).

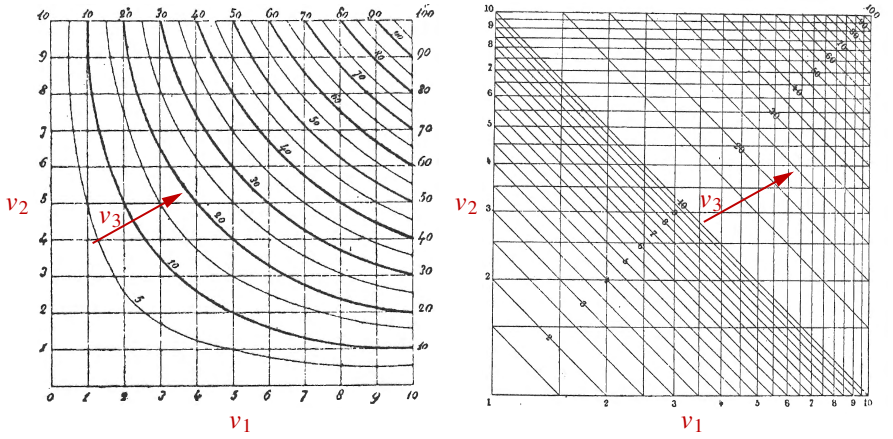

(a) Intersection nomogram.

(b) Intersection nomogram with logarithmic scales.

(c) Alignment nomogram, first version.

(d) Alignment nomogram, second version.

Figure 1 For the same task (calculating the product of two variables, which corresponds to the equation $F = v_3 - v_2 v_1 = 0$) different charts can be provided, with an alignment nomogram offering perhaps the most elegant solution. Notice that this can be drawn in different ways; the one in Fig. 1d has two linear scales (which are easier to draw). Charts reproduced from (d'Ocagne, 1899), with some changes for clarity.

We note that d'Ocagne's role has also been a matter of debate: some of his contemporaries, such as French geophysicist Charles Lallemand (1857–1938) and engineer Rodolphe Soreau (1865–1935) resisted the new terminology, arguing that nomograms were merely an extension of abacs (Soreau, 1902). However, we argue that the contributions by d'Ocagne, especially the application of projective geometry, were substantial, therefore introducing an essentially novel tool (Tournès, 2003, pp. 73–74).

After the publication of his seminal book, D'Ocagne greatly helped to popularize his invention through many later works, in which he presented example nomograms for several applications, such as physics, hydraulics, topography, navigation (Fig. 2), aviation and accounting (Tournès, 2003). By the 1920s, nomograms had become the main research topic in graphic computing (Tournès, 2000, p. 142, Fig. 3); moreover, they were the object of research interest also for their mathematical properties. For example, German mathematician David Hilbert, in his famed list (Hilbert, 1901) of 23 important open problems in mathematics, posed the 13th one in terms of nomographic

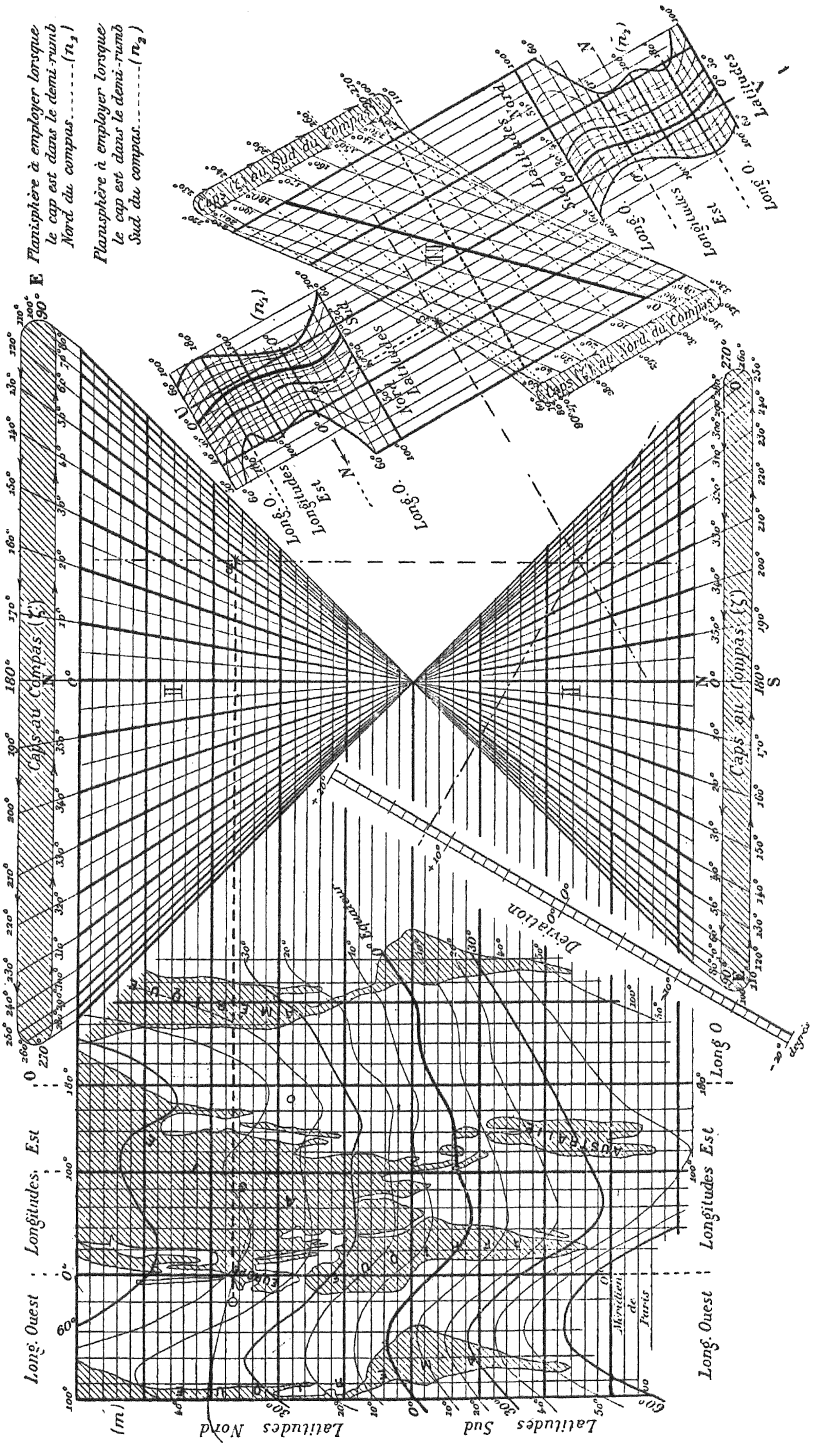

Figure 2 An example from (d'Ocagne, 1899) of a complex nomogram, to compute the deviation of a compass on a ship depending on the latter's geographic coordinates.

analysis, by asking whether a 7th-degree polynomial equation, which cannot be solved in closed form through algebraic functions, can be solved instead through nomograms. A solution was found by d'Ocagne himself; however, the solution required a movable element in addition to a nomogram and was thus deemed unsatisfactory by Hilbert, who conjectured that the problem could not be solved in nomographic terms. Hilbert's conjecture was finally disproved in 1957 (Tournès, 2014) by Russian mathematicians Andrej Kolmogorov (1903–1987) and Vladimir Arnol'd (1937–2010).

Another research topic was to determine whether a given equation of three variables can in fact be solved through nomograms, and if so, to find a procedure for creating them: this problem was finally solved in a practical form by Polish mathematician Mieczyslaw Warmus (1918–2007), who also presented (Warmus, 1959) a classification of the functions that can be written in nomographic form into seven principal cases.

By the 1950s, research in nomography, at first mostly published in French (Tournès, 2000, p. 141, Fig. 2) after the pioneering works by Pouchet, Lalanne and d'Ocagne, had become of interest at the global level; one can observe, for example, a significant amount of works by authors from the former Soviet Union (Evesham, 1986).

2.2 Decline: 1960–1990

The research on nomography began to decline in the 1960s (Tournès, 2000, p. 140, Fig. 1), as computers became commonly used in academia and industry. Nevertheless, nomograms remained in use, and published papers frequently presented calculations in nomographic form for practical applications; books and papers were written on the art of nomography and its potential uses (Bond, 1948; Ferrara, 1940). Topics that saw a significant use of nomograms are the analysis of internal combustion engines, manufacturing technology, design of hydraulic systems and civil engineering (especially for the study of soil mechanical properties). In all these cases, one needs to work with complex relationships that are often approximations of numerical data, thus the reduction in accuracy for a graphical approach (with respect to an analytic one) is not an issue. On the other hand, the possibility of quickly obtaining a result that can be used even in field work makes nomograms appealing for these applications.

Regarding applications in Machine Mechanics, we observe that until the '70s nomographic solutions for mechanism design problems were appreciated for their practicality: indeed, mechanism design generally leads to complex equations in which it is convenient to explore different design solutions, by designating different parameters as outputs. In particular, (Adams, 1960) developed a nomogram to optimize a four-bar linkage for function generation and observed how, after some practice, one can arrive in a relatively short time at a suitable solution with acceptably small errors. As it was common, the nomogram was available in large format on graph paper for practical use.

Other nomograms were developed during this period specifically for mechanism design; for instance, planar four-bar mechanisms were studied in (Antuma, 1978; Wunderlich, 1980), while (Meyer zur Capellen, 1983) considered their spherical equivalents. A planar mechanism with a contact pair, namely a cam-follower linkage, was studied in (El-Shakery & Terauchi, 1984) with the goal of preventing undercut. We also cite (Éidinov et al., 1976), on the vibration analysis of a spatial (Hooke's) joint.

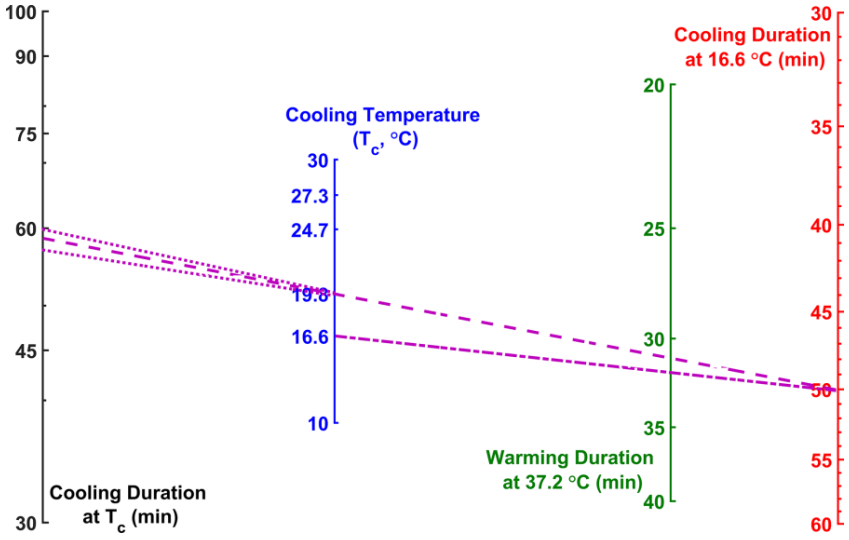

Figure 3 Nomogram for the design of a thermal therapy protocol for soft tissue injuries. The dotted lines on the left delimit the uncertainty zone for the result. Reprinted with permission from (Khoshnevis et al., 2018).

Nomograms proved useful also in the design of gears (Seireg & Houser, 1970; Wellauer & Holloway, 1976), to present large amounts of experimental data in a form that is more convenient for designers than numerical tables. Some applications were also proposed for vibration analysis (Hohenberg, 1967; Miconi, 1987).

2.3 Resurgence? 1990–today

After the '90s, nomograms have largely disappeared from engineering research, having been replaced by software that can be easily distributed. Nevertheless, nomograms are still present in published literature: for instance, they are still used in design standards and manufacturers' catalogs, to present results in a compact way. A common example is the Smith chart (Howison, 2014), used in electrical engineering for the design of transmission lines: in its essence, this graphical tool is again a nomogram.

Outside of engineering, nomograms have also had a significant impact on medicine (Grimes, 2008; Kattan & Marasco, 2010; Khoshnevis et al., 2018); see the example in Fig. 3. Nomograms are also used to quickly compute the BMI of a patient (Glasser & Doerfler, 2019). Their use in medicine is in fact somewhat controversial; however, even in a review (Grimes, 2008) that strongly criticized their usage as anachronistic, the author admitted that nomograms were undergoing a "resurgence", with more than 150 citations on the PubMed database in 2007 alone. Nomograms, indeed, can be helpful in explaining a complex situation to a patient (Kattan & Marasco, 2010), especially in comparison to PC programs, which may be perceived as less transparent. Nomograms are also low-cost and easily protected from environmental damage (by using waterproof paper); moreover, they allow users to compute results in emergency situations. These advantages can also be useful for engineers in some industrial applications.

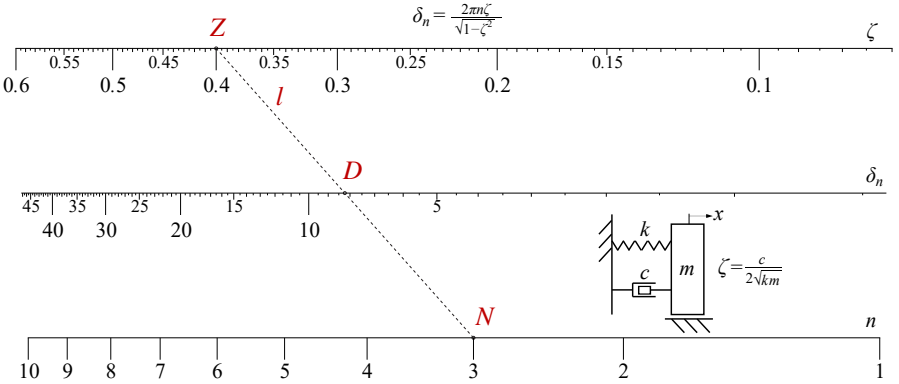

Figure 4 Nomogram for the logarithmic decrement δ_n of a mass-spring-damper system, defined as $\delta_n = \log(x_1/x_{n+1})$, where x_i is the amplitude of the i-th oscillation after release from an initial displacement (without external forces). Points Z, D and N are defined by the values $\zeta = \frac{c}{2\sqrt{km}}$ of the damping ratio, δ_n of the decrement and n of the number of oscillations for defining δ_n, respectively (each on the corresponding scale); c, k and m are the damping coefficient, the stiffness and the mass. The points are aligned on line l.

Finally, nomograms can still have a place where speed is of the essence: for example, they are used to predict the behavior of forest fires or the lift of hot-air balloons (Glasser & Doerfler, 2019). Another relevant application is artillery, in which nomograms were in standard use up to World War I (Hankins, 1999). Nomograms have also been proposed for estimating seismic hazard (Douglas & Danciu, 2020).

Considering the field of Machine Mechanics and Design over the last 30 years, we found several works on nomograms for gear train design (Esmail & Hussen, 2010; Esmail, 2013, 2016; Esmail et al., 2018); they are also still used for the design of planar (Hassaan, 2015) or spherical (Hwang & Chen, 2007; Lu, 1999) linkages, for optimizing motion laws in cams (de Freitas Avelar et al., 2021), for the analysis of the efficiency of a kinematic chain (Aleksandrov, 2011), for studying tire dynamics in a vehicle (Zotov & Balakina, 2007), and for the design of hollow springs (Bagaria et al., 2017).

3 Nomograms: methods and properties

In this Section, we briefly describe how nomograms can be drawn, using modern tools, for a few example problems in Machine Mechanics. While a complete guide on drawing nomograms (Doerfler, 2009) is beyond the scope of this work, we believe that some example nomograms can effectively show the advantages and limitations of these tools.

3.1 Modern nomographic tools: pyNomo

Traditionally, a notable limit of nomograms is that they require considerable skill in their design, not to mention the time needed to manually draw them in high detail. Recently, however, some software tools have been presented (Howison, 2014) that allow us to automate nomogram design: these tools can help reintroduce nomography in practical usage. Indeed, as observed in (Kattan & Marasco, 2010), it is desirable to have a tool that *"combines computerization with classical nomograms"*. At the time

of writing, the most complete software for this task (that we are aware of) is pyNomo (Boulet et al., 2020), a library for nomography written in the Python programming language. Therefore, we have created a few nomograms with pyNomo to illustrate some basic concepts in Machine Mechanics. A pyNomo script, once it has been run, generates and automatically compiles (through Python) a LaTeX source-code file; the final output is a PDF file containing the nomogram in high-quality vector graphics.

3.2 Selected nomogram types

In this work, we refer to the classification in the pyNomo documentation (Boulet et al., 2020), whose authors identify 10 types of nomograms (Martínez-Pagán & Roschier, 2022). Traditionally, the most common nomogram is the one defined by three parallel[2] straight lines (Type 1 in pyNomo[3]); an example of this design is in Fig. 4. The most general mathematical expression for an alignment nomogram, as defined in Eq. (3), becomes simpler in this case: having defined a coordinate system with axis x parallel to the scales, the j-th scale (along the line $y = y_j$) starts at $x = x_{jS}$ and ends at $x = x_{jE}$ ($j = 1, 2, 3$), therefore we can write

$$\begin{cases} f_{jx}(v_j) = x_{jS} + \Delta x_j g_j(v_j) \\ f_{jy}(v_j) = y_j \quad \text{(constant)} \end{cases} \quad \text{with} \quad \begin{cases} g_j(v_{jS}) = 0 \\ g_j(v_{jE}) = 1 \end{cases} \quad \text{and} \quad \Delta x_j = x_{jE} - x_{jS} \tag{4}$$

where $v_j \in [v_{jS}, v_{jE}]$ is the j-th variable, defining a point on the corresponding scale, and g_j is a suitable monotonic continuous function; for example, setting $g_j(v_j) = \frac{v_j - v_{jS}}{\Delta x_j}$ defines a uniform linear scale. Substituting in Eq. (3), one has

$$(y_3 - y_2)\,\Delta x_1 g_1(v_1) + (y_1 - y_3)\,\Delta x_2 g_2(v_2) + (y_2 - y_1)\,\Delta x_3 g_2(v_3) + C_0 = 0 \tag{5}$$

where C_0 is a constant depending on the parameters of the nomogram. This shows that any *weighted sum* of functions g_j can be computed with a nomogram such as the one shown in Fig. 4; the weights $(y_i - y_k)\,\Delta x_j$ for the summands can be set to a desired value by a proper choice of the start and of the end point for each scale.

A *product* of functions can also be computed with a Type 1 nomogram. For example, consider again the equation $F = v_3 - v_1 v_2 = 0$ (see Sec. 2.1), from which one has $v_3 = v_1 v_2$ and then $\log(v_3) = \log(v_1) + \log(v_2)$, after taking the logarithm of both sides. This is a special case of Eq. (5), where all three g_j's are logarithmic functions.

As an example, in Fig. 4 we show a nomogram that we developed to compute the *logarithmic decrement* δ_n for a one-Degree-of-Freedom (1-DoF) harmonic oscillator, namely a system with a mass m (translating along a line) connected to a fixed frame through a spring of stiffness k and a viscous damper of coefficient c, with the spring and the damper acting in parallel. The logarithmic decrement is a classical topic in Mechanics of Vibrations and is commonly presented in undergraduate courses. From

[2] In most nomograms of this type, the lines are vertical, for clarity. Here the lines are horizontal, to save space.
[3] In this paper, we follow the same terminology and classification proposed in (Boulet et al., 2020), for clarity.

the definition of δ_n and known results on free vibrations of such systems, one finds

$$\delta_n = \log\left(\frac{x_1}{x_{n+1}}\right) = \frac{2\pi n\zeta}{\sqrt{1-\zeta^2}} \tag{6}$$

from which one has

$$\log(\delta_n) = \log(2\pi) + \log(n) + \log\left(\frac{\zeta}{\sqrt{1-\zeta^2}}\right) \tag{7}$$

Adding $\log(2\pi)$ to the logarithms of the input values in Eq. (7) is "embedded" in the way the scales have been drawn in Fig. 4, which is possible since $\log(2\pi)$ is a constant value, and does not complicate the nomogram. An isopleth has been added to show how a computation is performed[4]: for $\zeta = 0.4$ and $n = 3$, one has $\delta_n = 8.23$, which is found by drawing a straight line l over the points Z and N in Fig. 4 and finding the intersection D of l with the scale for δ_n. In a practical application, one generally finds δ_n by directly measuring the amplitudes of vibration x_1 and x_{n+1} at two time instants which are n oscillations apart, then applying the definition on the left-hand side in Eq. (6); the goal is then to derive the damping ratio ζ, which is otherwise difficult to measure. Notice that, while inverting Eq. (6) analytically to obtain ζ as a function of δ_n may be not immediate for a student, solving the inverse problem with the nomogram is just as easy as solving the original direct problem of computing δ_n from ζ.

The same equation can be represented in nomographic form in different ways. For example, another possible representation of a product of two variables $v_3 = v_1 v_2$ is given by an "N" (also called "Z") type nomogram, which is classified as Type 2 in (Boulet et al., 2020): see for example Figs. 1c and 1d. Unlike a Type 1 nomogram, this latter design requires only one logarithmic scale (see again Fig. 1d). Let us consider three scales for the variables v_i, each starting at point $P_{jS} = (x_{jS}, y_{jS})$: this point corresponds to $g_j(v_j) = 0$. The direction of each scale is defined by vector $(\Delta x_j, \Delta y_j)$, which we assume to have unit magnitude, for simplicity. Equation (4) becomes

$$\begin{cases} f_{jx}(v_j) = x_{jS} + \Delta x_j g_j(v_j) \\ f_{jy}(v_j) = y_{jS} + \Delta y_j g_j(v_j) \end{cases} \quad \text{with} \quad g_j(v_{jS}) = 0 \quad \text{and} \quad \sqrt{\Delta x_j^2 + \Delta y_j^2} = 1 \tag{8}$$

while Eq. (3) in this case writes as

$$\begin{vmatrix} x_{1S} + \Delta x_1 g_1(v_1) & y_{1S} + \Delta y_1 g_1(v_1) & 1 \\ x_{2S} + \Delta x_2 g_2(v_2) & y_{2S} + \Delta y_2 g_2(v_2) & 1 \\ x_{3S} + \Delta x_3 g_3(v_3) & y_{3S} + \Delta y_3 g_3(v_3) & 1 \end{vmatrix} = 0 \tag{9}$$

If the scale for variable v_2 passes through P_{1S} and P_{3S}, and if the scales for v_1 and v_3 are parallel, it can be shown that linear scales can be set for v_1 and v_3, such that $g_1(v_1)$ and $g_3(v_3)$ are linear functions and that it holds $v_3 = v_1 v_2$. Since the only nonlinear scale is the one for v_2, the resulting nomogram is simpler to draw and, in some cases,

[4]No units of measurement are reported here, since all parameters n, ζ and δ_n involved are dimensionless.

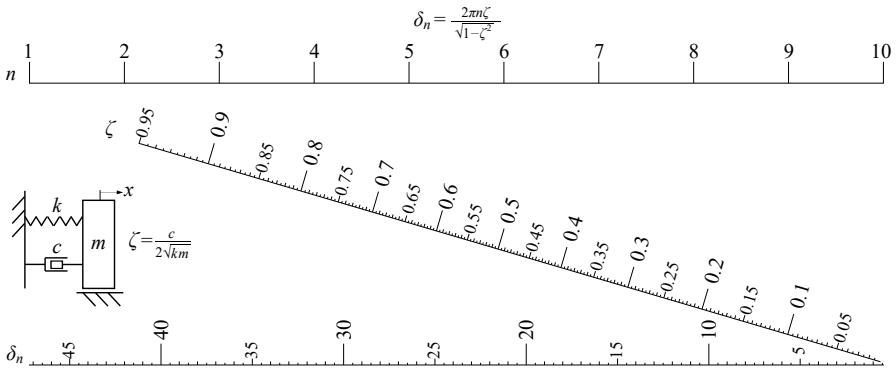

Figure 5 Again on the logarithmic decrement δ_n, this time using a Type 2 nomogram (compare with Fig. 4).

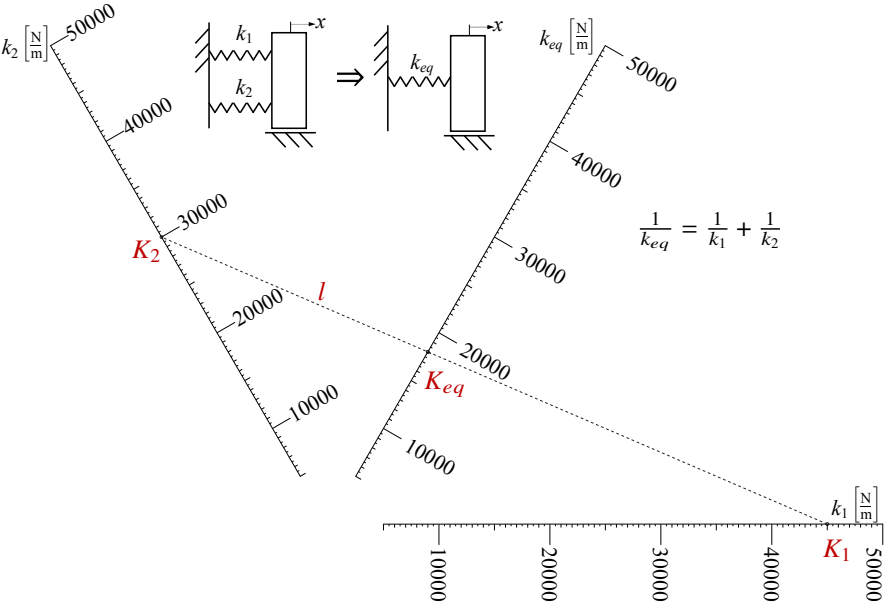

Figure 6 Nomogram for the stiffness k_{eq} of a spring, equivalent to two springs in series having stiffnesses k_1 and k_2, respectively. Here, all three scales have the same units of measurement and the same unit length.

more compact than the equivalent Type 1 nomogram for the same equation (obtained by using logarithmic scales, as previously explained). As an example, we have drawn another tool for computing the logarithmic decrement δ_n, but in this case by a Type 2 nomogram: the result is shown in Fig. 5. The fact that two of the scales are linear, while the one for ζ is only slightly deviating from linearity, arguably makes the resulting nomogram easier to read than the one in Fig. 4; notice that this nomogram also allows us to display a longer range for the scale corresponding to the variable ζ.

Yet another design is the "concurrent scale" (or "angle") nomogram: an example is shown in Fig. 6. This kind of nomogram, classified as Type 7 in (Boulet et al., 2020),

is defined by three scales passing through a common point, which for simplicity is taken at the origin of all three scales: therefore, at point $P_{1S} = P_{2S} = P_{3S}$ it holds $g_1 = g_2 = g_3 = 0$. The origin O of the coordinate frame is also set at the same point. Having defined the angle α_j of the j-th scale with respect to the x-axis, one has

$$\frac{\sin(\alpha_3 - \alpha_2)}{g_1(v_1)} + \frac{\sin(\alpha_1 - \alpha_3)}{g_2(v_2)} + \frac{\sin(\alpha_2 - \alpha_1)}{g_3(v_3)} = 0 \tag{10}$$

One application for this kind of nomogram that is of interest for Mechanics of Machines is computing the equivalent total stiffness of a system of two linear springs attached in series, having stiffnesses k_1 and k_2, respectively. It can be shown that the resulting system is statically equivalent to a single spring of stiffness k_{eq}, having

$$\frac{1}{k_{eq}} = \frac{1}{k_1} + \frac{1}{k_2} \tag{11}$$

This equation can be directly implemented in a Type 7 nomogram: see Fig. 6. Here, the isopleth l has been drawn for an example calculation with $k_1 = 45000\ \mathrm{N\,m^{-1}}$ and $k_2 = 30000\ \mathrm{N\,m^{-1}}$, corresponding to points K_1 and K_2, respectively; the resulting equivalent stiffness $k_{eq} = 18000\ \mathrm{N\,m^{-1}}$ is found at point K_{eq}, on the intersection of l with the third scale. Notice that unrealistic cases with either $k_1 = 0$ or $k_2 = 0$ are excluded by design: it is thus impossible to obtain incorrect results due to misreading the input. The angles α_j can be chosen according to our preference; if $\alpha_3 - \alpha_2 = \alpha_2 - \alpha_1 = 60°$, as in Fig. 6, all scales conveniently have the same unit length.

Finally, we discuss the Type 4 (or "proportion") nomogram (Boulet et al., 2020). A remarkable feature of this design is that it allows us to solve equations in *four* variables, instead of *three* as in the other types. Therefore, the corresponding equation cannot be written in the form shown in Eq. (3); nevertheless, this is still an alignment nomogram and its equation can be written in determinant form, for example as

$$\begin{vmatrix} 1 & 0 & 0 \\ 0 & f_1(v_1) & f_2(v_2) \\ 0 & f_3(v_3) & f_4(v_4) \end{vmatrix} = 0 \tag{12}$$

which is equivalent to

$$\frac{f_1(v_1)}{f_2(v_2)} = \frac{f_3(v_3)}{f_4(v_4)} \tag{13}$$

Figure 7 shows how such a nomogram is used: suppose that the v_2 (corresponding to the scale on the right) is the unknown which we seek as the output of the graphical computation, while v_1, v_3 and v_4 are known input parameters. We then draw a line through the points for v_4 and v_3 (corresponding to the top and the bottom scale, respectively), which intersects the auxiliary line at 45° with respect to the horizontal at a point A: we then draw a second line through A and the point for v_1, which intersects the scale on the right in a point corresponding to the value for v_2 which solves Eq. (13).

While Type 4 nomograms are more flexible, in our experience a significant drawback is in that they make it difficult for the designer to properly choose the ranges

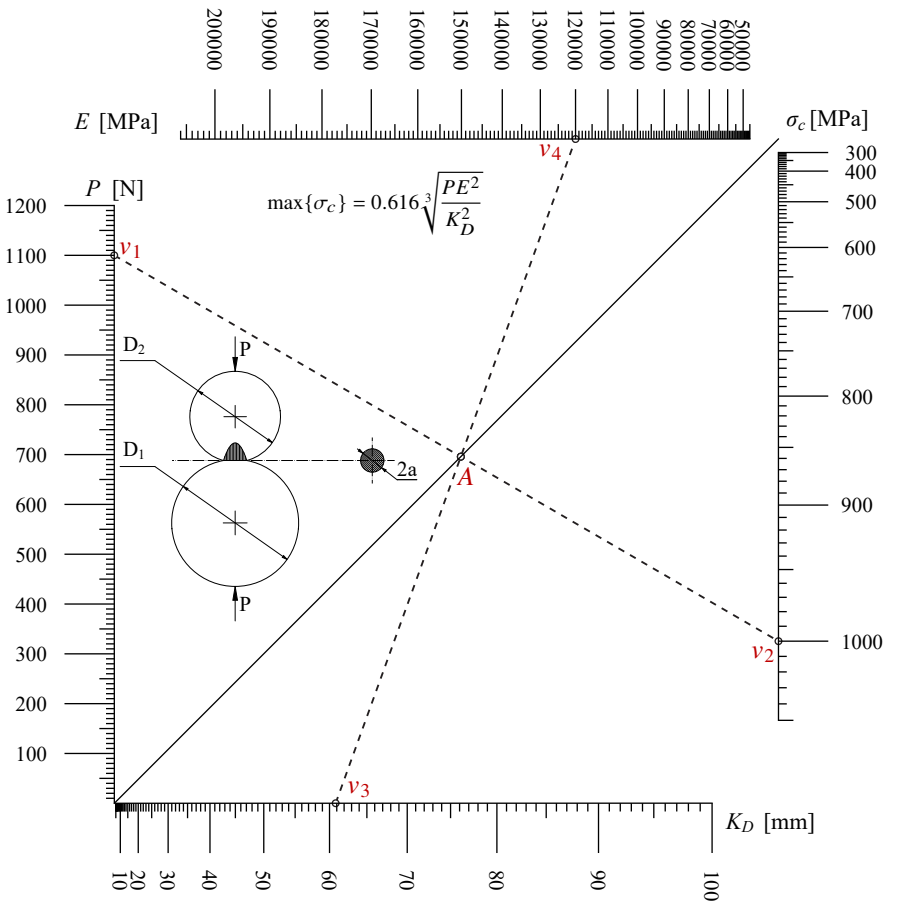

Figure 7 A Type 4 nomogram for computing the maximum Hertzian compressive stress between two balls, respectively having diameters D_1 and D_2, kept in contact by a force P; the contact area is a circle of diameter $2a$. We assume that the material is the same for both spheres and that it has a linear elastic behavior, defined by the constant parameters E (the Young's modulus) and $\nu = 0.3$ (the Poisson's ratio).

for each scale. In general, the choice of the minimum and maximum values to display in each scale significantly affects the readability and usefulness of the nomogram: in a practical case, realistic values are suggested by experience, but if the resulting scale is too long or too short it becomes difficult to find the desired value. In a Type 4 nomogram, this is complicated by the fact that the scales are interdependent.

As an example, we refer the reader to Fig. 7, a nomogram which we designed to analyze the Hertzian contact stresses between two elastic curved bodies: this is another common topic in Applied Mechanics courses which frequently leads to rather complex equations which lack an immediate physical interpretation. Considering in particular two elastic spheres composed of the same material, pushed against each other by a contact force P along the common axis between the centers of the spheres, the

maximum compressive stress σ_c in the zone of contact is (Young & Budynas, 2002)

$$\max\{\sigma_c\} = 0.616\sqrt[3]{\frac{PE^2}{K_D^2}} \tag{14}$$

in which E is the Young's modulus of elasticity for the material, which is the same for both spheres; it is assumed that this material has ideal linear elastic behavior and that its Poisson's ratio is $\nu = 0.3$, which is a common value for both steel and aluminum alloys. The parameter K_D, which units of length, is given by (Young & Budynas, 2002)

$$\frac{1}{K_D} = \frac{1}{D_1} + \frac{1}{D_2} \tag{15}$$

where D_1 and D_2 are the diameters of the two spheres, respectively. Notice that this parameter could be computed with another nomogram, for instance with a Type 7 design: comparing Eq. (15) with Eq. (11), the similarities are apparent.

The resulting nomogram for Eq. (14) is shown in Fig. 7; a similar nomogram could be drawn to compute the radius a of the contact area, which is a circle in this case. Limit cases, such as the contact between a sphere and a plane (when one of the diameters D_i goes to infinity) can be still be analyzed through the same nomograms.

Considering more general cases, such as the spheres being composed of different materials, introduces other variables: therefore, one needs to combine multiple nomograms together, to compute intermediate terms. This is in fact one of the strongest advantages of alignment nomograms over, for example, lookup graphs: a few examples of more complex combined nomograms are presented in Sec. 4. The possibility of combining nomograms is already provided in the pyNomo library, which greatly simplifies the design. While nomograms provide an aesthetically pleasing, easy to read graphical tool, one of their drawbacks is that introducing more and more variables in an equation, to consider more general cases, quickly leads to unwieldy designs that are difficult to read and which must be printed in very large format for readability. In our experience, equations in more than eight independent variables become impractically complex for nomography: unless some special cases of interest can be defined, with some variables having fixed values (which reduces the number of scales in the design), other computing methods, such as software tools, should be used instead.

We conclude our discussion by noting that there are several designs in the literature that extend the concepts above and thus cannot be easily categorized. For instance, some nomograms use circular scales (such as the Smith chart), while others use more complex curves such as the *folium* of Descartes; with this design, some nomograms were devised for the product of two variables, where all three scales coincide (Doerfler, 2009; Evesham, 1986). When curved scales are used, more than one intersection point may be found, corresponding to different solutions (for nonlinear equations).

Equation (3) can also be generalized to contain up to six variables, as

$$\begin{vmatrix} f_{1x}(u_1, v_1) & f_{1y}(u_1, v_1) & f_{1z}(u_1, v_1) \\ f_{1x}(u_2, v_2) & f_{1y}(u_2, v_2) & f_{1z}(u_2, v_2) \\ f_{1x}(u_3, v_3) & f_{1y}(u_3, v_3) & f_{1z}(u_3, v_3) \end{vmatrix} = 0 \tag{16}$$

which is defined as a Type 9 nomogram in (Boulet et al., 2020; Martínez-Pagán & Roschier, 2022). In this case, each scale is replaced by a graduated grid in the two variables u_j and v_j, which define a point on the grid; the resulting nomogram is still defined by the alignment of three points (one for each grid). While more flexible, these nomograms easily lead to cluttered and hard to read designs, which goes against the spirit of having a readable tool enhancing the visualization of the results.

4 Applications of nomography

To illustrate concrete applications of nomography in the analysis of machines and mechanisms, we present a few example designs of more complex nomograms, devised to solve some practical problems. The first one, shown in Fig. 8, has been developed for the kinematic analysis of a spatial mechanism. This design has been inspired by a collaboration with a company working on variable-displacement axial piston pumps; a swashplate can be rotated by an angle α to control the displacement. The company reported a need to compute the pump displacement from direct measurements on its components: this is useful when working on a shop floor, as the pump data (such as the serial number and product specification) may not always be directly available. The displacement V can then be computed from easily measured quantities, as

$$V = \frac{\pi d^2}{4} Z D \tan(\alpha) \tag{17}$$

where d is the piston diameter, Z their number and α the swashplate inclination. The axes of translation of the pistons all lie on a (virtual) cylindrical surface of diameter D.

Clearly, Eq. (17) can be implemented in any computation software, for instance as a spreadsheet. However, operating a digital device when disassembling a pump (which is generally filled with lubricant) for maintenance operations is clearly inconvenient. Moreover, there is a significant risk of operator errors due to incorrect data entry.

Nomograms are an interesting option for this task. However, Eq. (17) contains five variables; thus, it cannot be directly expressed as a nomogram of one of the types presented previously. We then divide the nomogram design in three parts, as follows.

1. We create a nomogram to compute $A = \frac{\pi d^2}{4} Z$: this corresponds to the global cross-sectional area of the pistons. This is achieved through a simple Type 2 nomogram with three variables, as described in Subsec. 3.1, namely $v_1 = d^2$, $v_2 = Z$ and $v_3 = A\frac{4}{\pi}$: the product $v_3 = v_1 v_2$ is on the auxiliary scale denoted by A in Fig. 8.
2. The result from the previous nomogram is used in the second step, by joining the two nomograms at the scale A; this second nomogram computes $V_0 = DA$. Again, having a product of two variables, a Type 2 nomogram is used here.
3. Finally, a third nomogram is introduced, joined with the previous one at the scale for V_0. This gives $V = V_0 \tan(\alpha)$, namely the displacement for each pump rotation.

The final result is shown in Fig. 8; here, the two vertical scales in the middle correspond to variables A and V_0, respectively. The numerical values of these intermediate quantities are not required by the user; thus, no ticks are displayed, to avoid cluttering

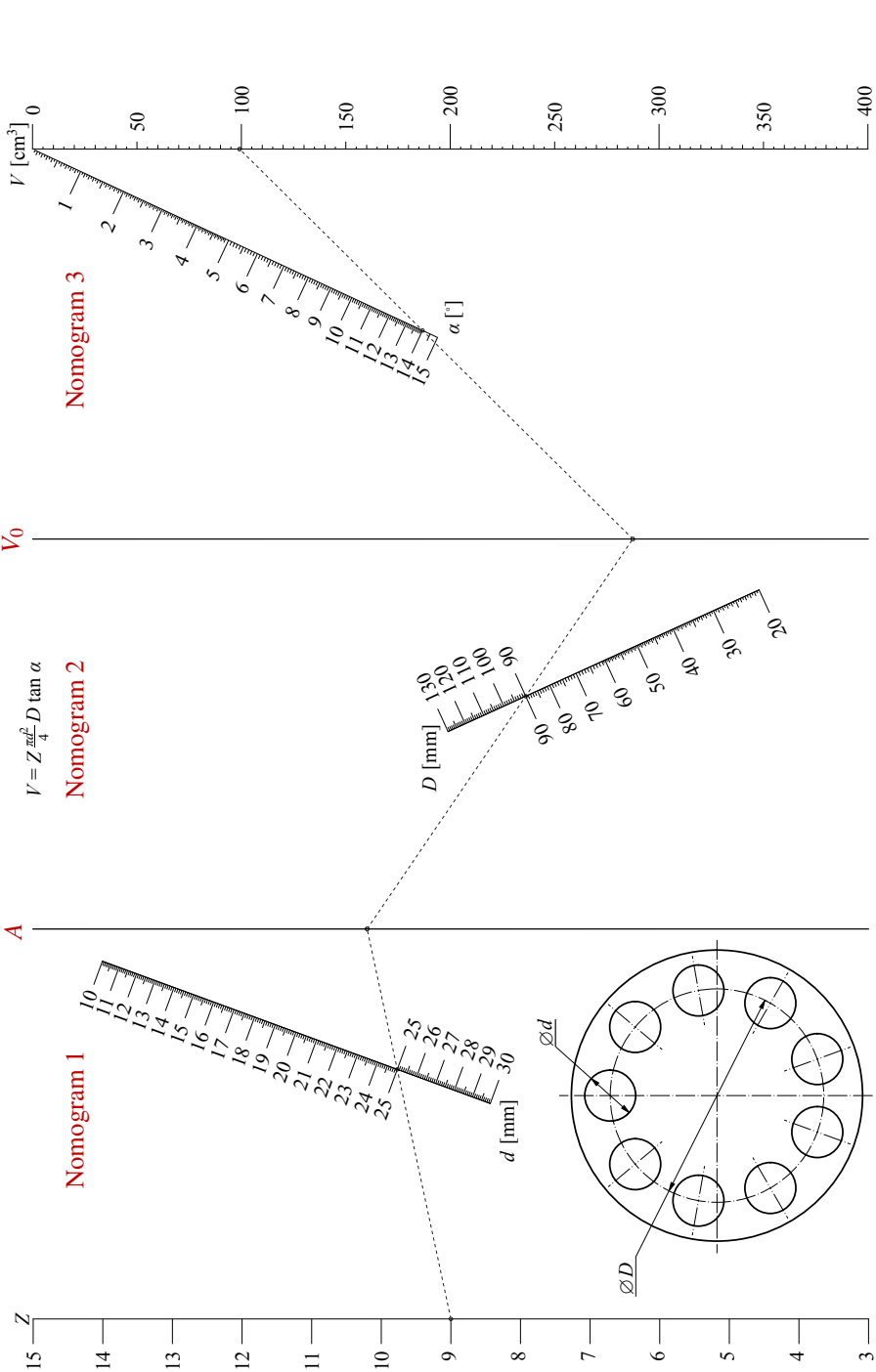

Figure 8 A combined nomogram (composed of three "intermediate" Type 2 nomograms) for calculating the displacement of a volumetric axial piston pump with a swashplate.

the graph. The isopleth on the graph shows an example calculation for a realistic pump design; on one corner of the nomogram, a sectional view of the central cylinder block of the pump is shown for reference, to clarify the definitions of diameters D and d.

This nomogram can be printed on laminated paper, to protect it from oil spills, and introduced in shop-floor practice for quick computations. The isopleths at each step can be found with a rigid element having a straight-line segment of sufficient length.

We also suggest applications for educational purposes. As noted in (Doerfler, 2009; Douglas & Danciu, 2020; Kattan & Marasco, 2010; Martínez-Pagán & Roschier, 2022; Tournès, 2003), nomograms allow the user to easily understand the properties of equations with complex algebraic expressions; also, nomography is a graphical approach that makes it unlikely to misinterpret inputs or results. Besides nomograms, other graphical methods, such as those used for planar mechanism kinematics and statics, are currently taught in mechanical engineering courses. While these methods could be replaced with purely analytical approaches, they are still used due to their pedagogical value. We thus expect nomograms to easily fit in existing courses; in particular, nomography extends graphical approaches for computation to any equation that can be written in determinant form as in Eq. (3). Some personal experiences on nomograms for math education in high schools were reported in (Tournès, 2018); a test on their usefulness for university-level education would then be worthwhile to understand their strengths and limitations. We also believe that mentioning examples of nomograms, together with their uses and applications, within a course in Mechanics of Machines, could also enhance interest among students in historical methods for engineering analysis and in its broader historical development.

For the reasons outlined above, we devised a few nomograms on topics frequently discussed during a course on Mechanics of Vibrations. The first one is shown in Fig. 9 and it has been developed to compute the first resonance frequency f of an inextensible taut string. This is usually the first example presented to the students of a *continuous* vibrating system, namely an element which has infinitely many DoFs and thus an infinite number of resonance frequencies. Under the usual assumption of small vibrations with respect to the equilibrium configuration (namely, with the string on a straight line segment), the first natural frequency is (Young & Budynas, 2002)

$$f = \frac{1}{2l}\sqrt{\frac{T}{\rho}} \tag{18}$$

where l is the length of the string from one fixed attachment point to the other, T is the string tension and ρ its linear density; it is assumed that the string has uniform section and that it can only withstand tensile forces (that is, it has zero flexural stiffness).

As shown in Fig. 9, since Eq. (18) contains four variables, the nomogram can be obtained by combining two simpler Type 2 nomograms. The final result, namely the vibration frequency, is shown on the rightmost scale. An interesting feature of nomograms is that two different scales can be accommodated along the same line, for instance to convert results between different units of measurement: indeed, the frequency in Fig. 9 is reported both in hertz and with the corresponding musical note

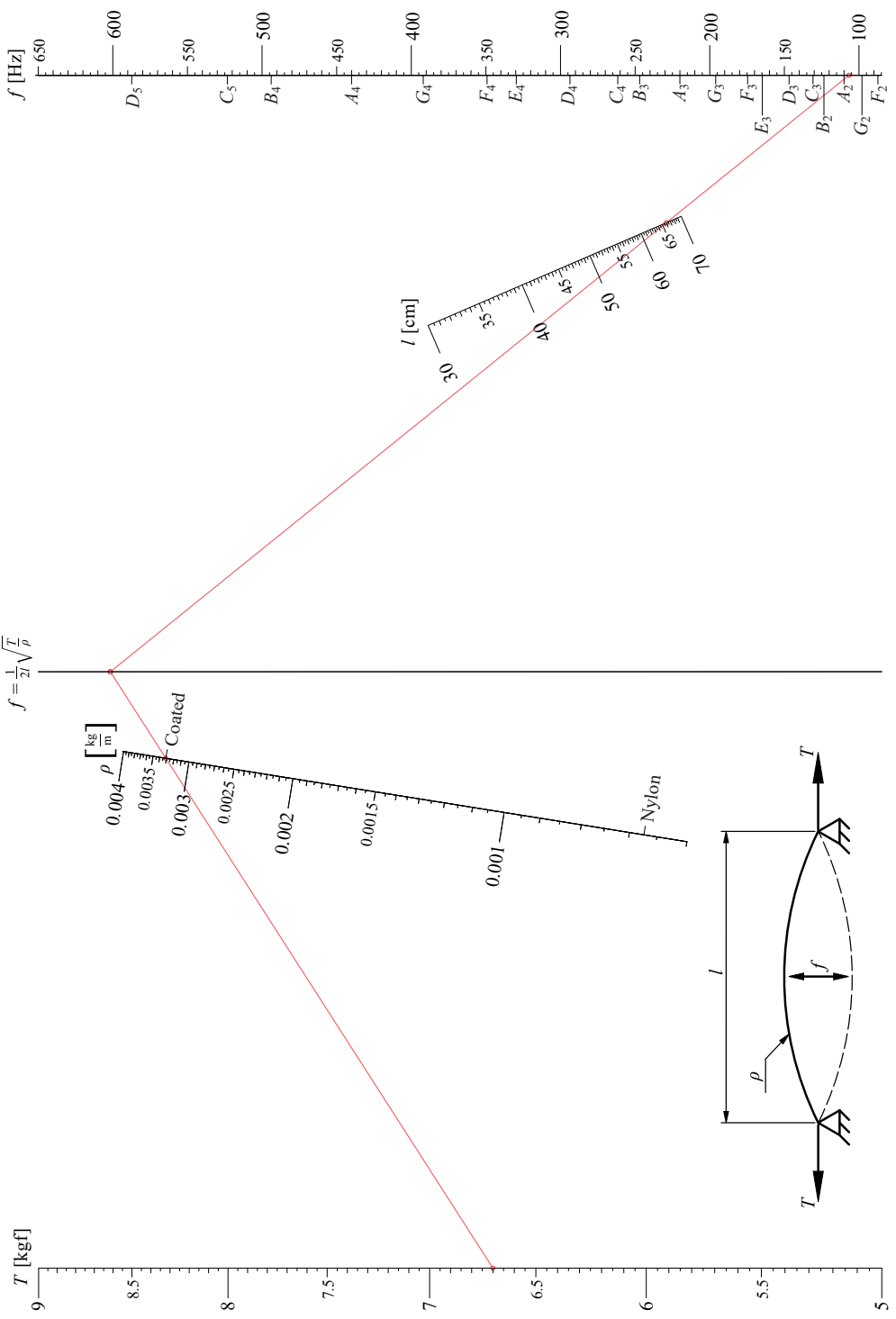

Figure 9 A combined nomogram (composed of two Type 2 nomograms) for calculating the first natural vibration frequency of a guitar string and the corresponding note.

(expressed in the international pitch notation). This increases the educational value of the nomogram in the classroom, as it allows to directly link the numerical result to something that the students (at least, those with some musical training) may understand more immediately; this link is otherwise far from obvious when looking at Eq. (18). This nomogram has indeed been developed by considering a musical instrument (the classical guitar) as a reference: meaningful values, obtained from producers' catalogs, were defined for the string density, taking into account the different materials that can be used[5]. The corresponding values are reported on the scale for ρ. Similarly, the range for the length L and for the tension T has been derived from manufacturers' websites. Notice that the resulting range for f is somewhat unrealistic, as the maximum frequency D_5 obtained is too high for a classical guitar; this is due to a design choice, in which we consider all possible values for each of the input scales and compute the corresponding possible range for f (even considering the "extreme" case of maximum T and minimum l and ρ). This can be useful in a classroom, to explore the full set of possibilities for a theoretical formula such as Eq. (18); in a practical case, one may otherwise choose to artificially restrict some ranges according to data or personal experience, to exclude unrealistic values. An interesting exercise that could then be proposed to students is to consider a real guitar cord, with assigned values of ρ and l, and explore the full range of notes that can be achieved by changing the tension T, to obtain a deeper understanding of the influence of the input values on the final results.

Another nomogram that we developed for educational purposes is presented in Fig. 10. Let us consider again the 1-DoF damped harmonic oscillator introduced in Sec. 3.1, for which we aim to find the *critical damping ratio*. This is the value c_{cr} which determines the behavior of the system under free vibrations: in particular, if the actual damping coefficient c is lower than c_{cr} there will be a damped periodic motion, otherwise the motion will be aperiodic and exponentially converging to the equilibrium position without oscillations. For a system having mass m and stiffness k, it holds

$$c_{cr} = 2\sqrt{km} \tag{19}$$

To provide a concrete example to the students, we assume that the compliance of the system is given by a rubber spring having cylindrical shape, as shown in Fig. 10; the spring design is defined by its height h, diameter d and by the Young's modulus E of the rubber. The stiffness is then found as (Young & Budynas, 2002)

$$k = \frac{\pi d^2 E}{4h} \tag{20}$$

Finally, we assume for simplicity a linear viscous behavior to model damping effects: thus, the damping force is given by $F_d = c\dot{x}$, where x is the displacement from the equilibrium position of the mass m and $\dot{x}$ is its velocity[6].

The nomogram for computing c_{cr} in Fig. 10 is obtained by combining two

[5]Usually, strings either made of Nylon or of steel-coated Nylon are used, respectively for the higher and the lower pitches.

[6]In a practical case, the viscous model is not strictly valid, as the internal hysteresis of the rubber should be taken into account; however, in an educational setting this would distract from the example and complicate the design of the nomogram.

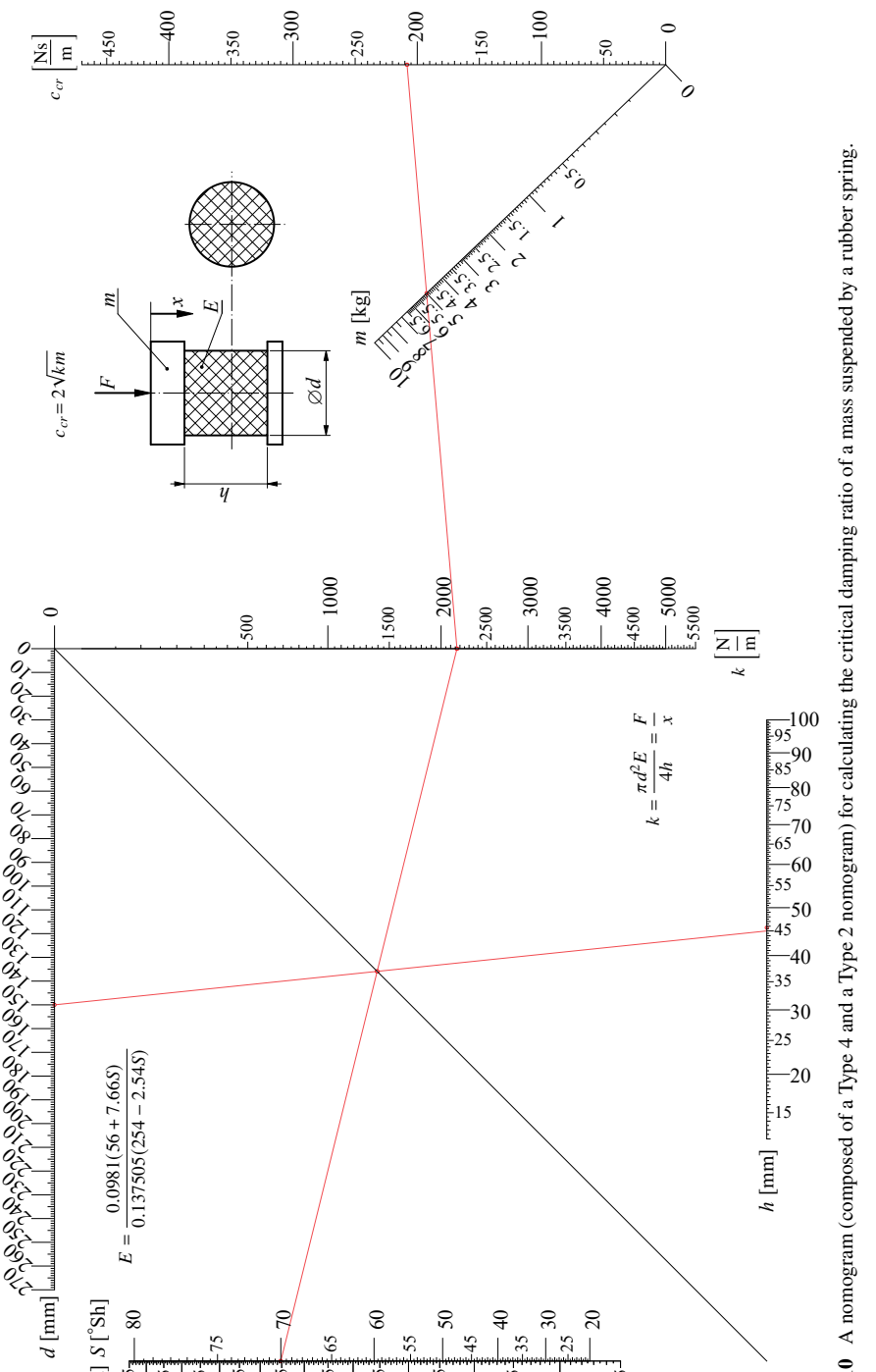

Figure 10 A nomogram (composed of a Type 4 and a Type 2 nomogram) for calculating the critical damping ratio of a mass suspended by a rubber spring.

nomograms, one (on the left) implementing Eq. (20) for the stiffness k, and the other (on the right) for solving Eq. (19) from the known values of k and m. In the first nomogram, two scales are reported to define the elastic properties of the rubber: indeed, while most manuals on Machine Design report Eq. (20) as a function of the elastic modulus, it is common in engineering practice to measure the hardness of rubber materials in Shore degrees (indicated as °Sh). These two parameters, however, are generally not independent, and several functions have been proposed for correlating them: here we take the one advanced in (Gent, 1958), which is expressed as

$$E = \frac{0.0981(56 + 7.66S)}{0.137505(254 - 2.54S)} \tag{21}$$

in which E is expressed in MPa and S is the rubber hardness (using a durometer according to the standard ASTM D2240 Type A). In a sense, this doubly-graduated scale can be seen as another nomogram, specifically an example of a Type 8 nomogram according to (Boulet et al., 2020; Martínez-Pagán & Roschier, 2022). This is a simpler nomogram with a single scale, graduated on both sides: this design allows us to compute functions in one variable $v_2 = f(v_1)$, by reporting the values for v_1 on one side of the scale and those for v_2 on the other side. The conversion in Eq. (21) is defined by a complex equation depending on numerical coefficients: it would then be easy to make a typing mistake when using a handheld calculator or reporting the formula in a spreadsheet. Using the nomogram in Fig. 10, on the other hand, is straightforward.

In this nomogram, as in Fig. 9, an isopleth has been drawn (with a thin red line) to illustrate an example calculation. A student may then explore the design alternatives and their effect on the final results, for instance by verifying how the coefficient c_{cr} changes depending on the type of rubber used for the spring (all other parameters being equal). The nomogram could also report on the leftmost scale some reference values of Shore hardness for common industrial rubbers, providing also practical guidance in the evaluation of realistic values for an example rubber which is yet to be tested.

As a last example, we present a nomogram that can be used in a design or research setting. An active topic of study in Machine Design is devising *statically-balanced mechanisms*, namely mechanical systems which are in a constant state of neutral static equilibrium under the effect of gravity. These devices are of practical importance in robotics (Mottola et al., 2022), where they can be used to compensate or at least reduce the torque at the motors due to the gravitational force, or in handheld tools such as lamps and desks, to reduce the effort required by the user to move the tool at the desired position. These mechanisms generally employ either counterweights or springs to balance the effects of the own weight of their links; the goal is to obtain a system which can move while maintaining constant (or almost constant) total energy

$$V_t = V_g + V_e \tag{22}$$

due to all conservative forces: these are introduced by gravity, whose contributions are grouped in the term V_g, and by the elastic elements, corresponding to term V_e. In the following, as it is commonly done in this area of research, we assume that all forces are in fact conservative: therefore, for example, we disregard frictional effects.

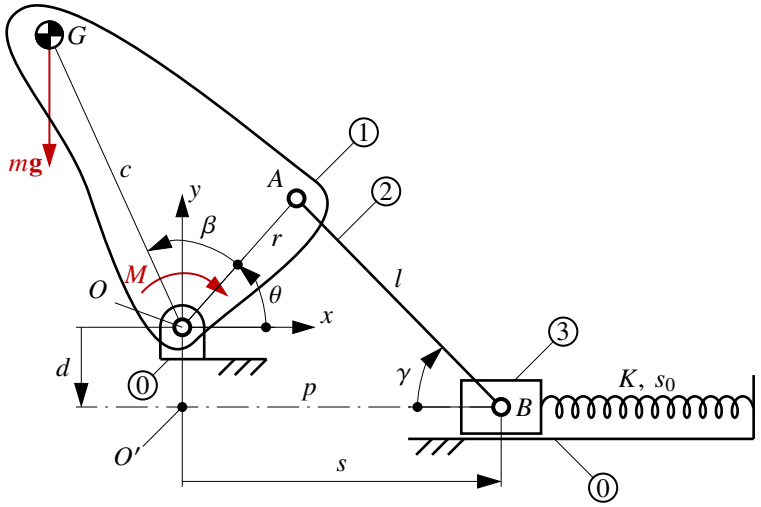

Figure 11 Schematic of a planar slider-crank linkage with a spring between links 0 and 3 for static balancing.

Let us now consider a 1-DoF system, such as the slider-crank planar mechanism shown in Fig. 11. Here, the crank 1 revolves around the fixed frame 0 around a revolute (R) joint in point O, and is connected to the coupler 2 with an R joint in A; finally, the slider 3 is connected with another R joint in point B to the coupler, and translates along axis p of a prismatic (P) joint with respect to the frame. A reference point O' is defined at the projection of O along p. All links are assumed to be perfectly rigid; the motion takes place in the vertical plane under the effect of gravity. The kinematic equations are found from the loop-closure constraint on $OABO'$: considering its components along the x and y axes (which define a coordinate system with origin in O), we obtain

$$\begin{cases} s = l\cos(\gamma) + r\cos(\theta) \\ d = l\sin(\gamma) - r\sin(\theta) \end{cases} \tag{23}$$

with $s = \overline{O'B}$, $l = \overline{BA}$, $r = \overline{AO}$, and $d = \overline{OO'}$; angle θ is defined between segment OA and the horizontal x axis, while $\gamma = \widehat{O'BA}$. Without loss of generality, we consider units of length such that $l = 1$. From Eq. (23), with algebraic manipulation one obtains

$$s = r\cos(\theta) + \sqrt{1 - [d + r\sin(\theta)]^2} = s(\theta) \tag{24}$$

The crank has its center of mass (CoM) in G, at distance c from O. The crank weight is $m\mathbf{g}$, where $\mathbf{g} = [0, -g]^T$ is the acceleration vector (with $g = 9.80665$ m/s^2); the masses of the other links are disregarded. The term V_g due to gravity in Eq. (22) is then

$$V_g = gc\sin(\theta + \beta) \tag{25}$$

where $\beta = \widehat{AOG}$; the mass m is assumed to be 1 in a suitable system of units.

An ideal (linear) spring of stiffness K is attached between the slider 3 and the fixed frame 0, to balance the weight of the crank. This spring stretches along axis p as the slider moves, and is at rest when $s = s_0$. Thus, the elastic potential V_e is

$$V_e = \frac{1}{2} K \, (s - s_0)^2 \tag{26}$$

We assume that the mechanism geometry, defined by r, c, β and d, is given and cannot be changed. We then seek the "best" spring, defined by parameters K and s_0, which minimizes the residual torque M that must be applied at O to balance the mechanism under static conditions (we disregard inertial effects): we then have

$$M(\theta) = \frac{d}{d\theta} V_t(\theta) = \frac{dV_g}{d\theta} + \frac{dV_e}{d\theta} = \underbrace{gc\cos(\theta + \beta)}_{M_g(\theta)} + \underbrace{\frac{1}{2} K \frac{d}{d\theta} \left[s(\theta) - s_0 \right]^2}_{M_e(\theta)} \tag{27}$$

in which we have made explicit the dependence of the energy V_t from Eq. (22) and of the torque M on the angle θ, which defines the configuration of the mechanism. If $V_t(\theta)$ is a constant, then $M(\theta)$ is always zero and the mechanism is in static equilibrium for a continuous range of configurations. Notice that, while the weight acting on the crank is constant, the corresponding torque $M_g(\theta)$ at O due to said weight is instead a nonlinear function of the position, which complicates the balancing.

In a practical case, however, perfect balancing may not be necessary: if the residual torque M is sufficiently small over the required range of motion $\theta \in [\theta_{min}, \theta_{max}]$, it can be acceptable to leave the mechanism partly unbalanced (Radaelli et al., 2011), as frictional effects generally help in maintaining static equilibrium. Otherwise, more complex balancing mechanisms may be added, such as cam-follower systems (Hain, 1961; Hilpert, 1968): the slider-crank mechanism can then balance most of the unbalance torque $M_g(\theta)$, while a cam-based linkage, which is usually more delicate, compensates the remaining smaller term while having to withstand smaller forces.

An application of the mechanism shown in Fig. 11 can be derived by fixing the crank 1 on a component which is to be balanced: G is then the global CoM of the components moving together, and m is the total mass of the crank and of the component to which it is attached. This design could be usefully applied, in robot arms or hand-operated devices: for example, similar concepts are known from the patent literature for hinges to be applied on furniture doors, to prevent them from slamming down.

Equation (27) could be studied analytically, in order to find a choice of K and s_0 that makes the right-hand term identically zero for all θ; however, we are not aware of previous exact results in this area. Here, instead, we suggest a mixed numerical-graphical method, whose application to statically-balanced mechanisms is novel, to the best of our knowledge. Our approach is as follows: we consider a set of possible mechanisms having the same schematic (Fig. 11), with each mechanism being defined by a combination of r, c, β and d (whose values are within given ranges of interest for the geometric parameters), and a range of rotation angles $\theta \in [\theta_{min}, \theta_{max}] = \Theta$. For

each element in the set, we solve the following optimization problem:

$$\min_{K>0,\, s_0 \in \mathbb{R}} \left(\max_{\theta \in \boldsymbol{\Theta}} M(\theta) \right) \tag{28}$$

and store the values of K_{opt} and $s_{0,opt}$ thus obtained. Then, we seek an interpolation function which approximates the optimal values of K and s_0 from the corresponding values of the geometric parameters: while in general this function will not provide the exact optimum, the error can be made reasonably small if the interpolating function is properly chosen. The approximation is also less of an issue here since even the optimal values do not, in general, provide an exact balancing. These approximate functions $K_{opt} = f_K(r, c, \beta, d)$ and $s_{0,opt} = f_s(r, c, \beta, d)$ can provide useful guidance to the designer, who will not have to solve the optimization problem in Eq. (28), which is nonlinear (and thus in general quite complex). Being approximations of numerical data, the functions f_K and f_s are in general complex to write and compute and contain approximate coefficients; thus, as seen for Eq. (21), which interpolates experimental data, a nomogram can speed up the computation and reduce the risk of errors.

The space of possible mechanisms is defined by four geometric parameters r, c, β and d, which leads to a rather complex nomogram. For simplicity, we now consider the important special case in which the offset d is zero, namely the in-line slider-crank. To further simplify the analysis, we then consider two extreme positions of the linkage, at $\theta + \beta = \frac{\pi}{2}$ and at $\theta + \beta = -\frac{\pi}{2}$. From Eq. (27), it is apparent that at these positions the torque $M_g(\theta)$ due to the gravitational term is zero. If we require having exact static equilibrium at least at these two positions, with no residual unbalance torque M, it follows that it must hold $M_e(\theta) = 0$, too; expanding Eq. (27), we find

$$M_e(\theta) = \frac{1}{2} K \frac{d}{d\theta} \left[s(\theta) - s_0 \right]^2 = \frac{1}{2} K \cdot 2 \left[s(\theta) - s_0 \right] \cdot \frac{d}{d\theta} s(\theta) \tag{29}$$

(recall that s_0 is a constant). In Eq. (29), K cannot be zero, as that would be equivalent to having no balancing spring; therefore, it must either be $s(\theta) = s_0$ or $\frac{d}{d\theta} s(\theta) = 0$. Since $s(\theta) = s_0$ cannot hold at both positions, we require the derivative of $s(\theta)$ to be zero: this condition defines the two limit positions of the mechanism, at the opposite extremes of the stroke. From this condition and simple geometry, it is easy to show that it must be either $\beta = \frac{\pi}{2}$ or $\beta = -\frac{\pi}{2}$; we then take the first condition in our design.

Having set $d = 0$ and $\beta = \frac{\pi}{2}$, we launched a numerical simulation, in which we explored all mechanisms in the ranges[7] $c \in [2, 18]$ and $r \in [0.05, 0.35]$. After discretizing the ranges of input geometric parameters, we then solved Eq. (28) for each mechanism and interpolated the resulting optimum values of K and s_0 as functions of c and r. For simplicity, we used a Type 2 nomogram such as the one in Fig. 5, which computes the product of two functions: we thus needed to interpolate the results as $K_{opt} = f_K(r, c) = f_{K1}(r) f_{K2}(c)$ and $s_{0,opt} = f_s(r, c) = f_{s1}(r) f_{s2}(c)$. As a compromise between accuracy and simplicity, we used 7$^{\text{th}}$ order rational functions for all functions f_{Kj} and f_{sj}; all the optimization and interpolation problems were

[7]The units are not reported, since these values actually correspond to the adimensional ratios c/l and r/l.

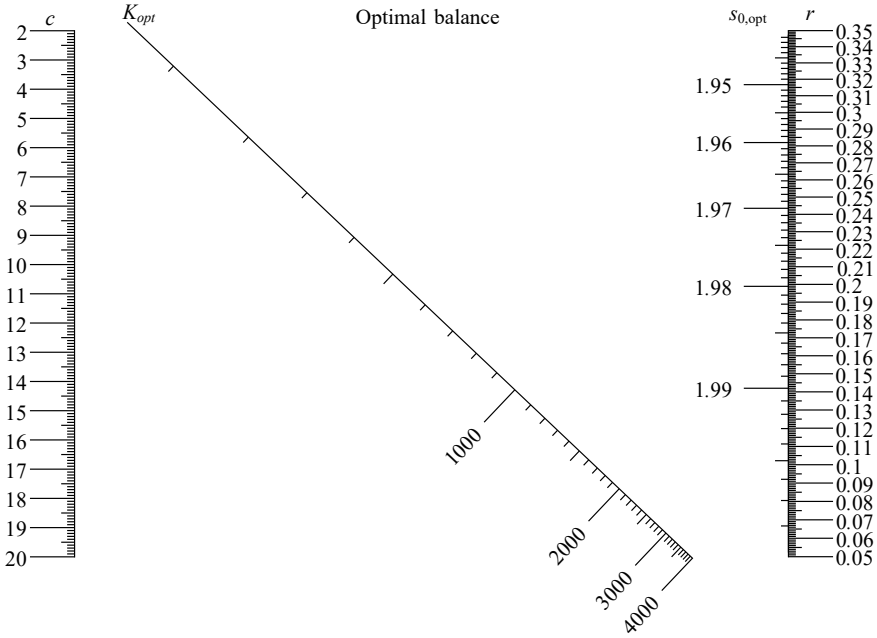

Figure 12 A nomogram for generating optimally-balanced slider-crank linkages; see also Fig. 11.

solved in MATLAB. We thus found

$$K_{opt} = g\frac{-128c(4+r^2)}{r(-512+64r^2+36r^4+5r^6)} \tag{30}$$

and

$$s_{0,opt} = \frac{1024-59.5r^4-6.94r^6}{124.7r^2+512.2} \tag{31}$$

The parameter c was found to have almost no influence on the optimal free length of the spring: thus, it does not appear in Eq. (31). The design in Fig. 12 is a combination of a Type 2 nomogram, to compute K_{opt} by implementing Eq. (30), and a Type 8 nomogram, to find $s_{0,opt}$ as a function in a single variable from Eq. (31).

The resulting mechanisms, while not perfectly balanced in general, are found to have very small residual unbalanced torques M: in the worst-case scenario among all mechanisms considered, the maximum value of M was reduced by 94.7% with respect to the corresponding maximum value without the balancing spring. While Eqs. (30) and (31) only provide approximations of the optimal design values, the errors with respect to the results from the optimization problem in Eq. (28) never exceed 0.1%.

A nomogram such as the one in Fig. 12 is thus found to be an effective design tool, which condensates a large mass of data in a simple schematic; it could then be applied by designers who need to apply the generic concept in Fig. 11 to several use cases, with no need to solve optimization problems (which usually require software packages that are vast and complex to use) nor to understand the finer details of the design equations.

5 Conclusion and future work

In this paper, we present a short history of nomography, a graphical computing method which used to be a common tool for both scientists and engineers. We thus discuss the ideation and development of this concept, together with a selection of its applications (especially in mechanical engineering); we also present a few example nomograms, together with their mathematical properties. Finally, we show some nomograms that we developed especially for educational and design purposes. In our research, we used pyNomo, an open-source library (under GPL3 license) which greatly facilitates the work of the nomographer: we thus find that software, which cause the progressive decline of interest in nomograms, can help in bringing renewed interest in these tools.

In future work, we aim to propose nomograms in educational settings, for instance within a course in Mechanics of Machines: this way, we may appreciate their actual effectiveness for didactic purposes. We also aim to develop some new nomograms for more complicated topics, such as Assur groups or matrices for 3D rotations, which frequently cause difficulties for the students. It is hoped that this work can also renew interest among researchers in the intriguing mathematical properties of nomograms.

Acknowledgments. The authors thank the chair and the Scientific Committee of the *"7th International Symposium on History of Machines and Mechanisms (HMM 2021)"* for selecting our previous conference paper (Mottola & Cocconcelli, 2022) to be revised and extended for publication in the present special issue.

Declarations

The authors declare no competing interests.

References

Adams, D. P. (1960). Nomographic synthesis of generator linkages. *J. Eng. Ind.*, *82*(1), 29–38. doi:10.1115/1.3662986

Aleksandrov, I. K. (2011). Determining the limiting efficiency of a kinematic chain. *Russ. Engin. Res.*, *31*, 539–540. doi:10.3103/S1068798X11060037

Antuma, H. J. (1978). Triangular nomograms for symmetrical coupler curves. *Mech. Mach. Theory*, *13*(3), 251–268. doi:10.1016/0094-114X(78)90049-6

Bagaria, W. J., Doerfler, R., & Roschier, L. (2017). Nomograms for the design of light weight hollow helical springs. *Proc. Inst. Mech. Eng., Part C*, *231*(23), 4388–4394. doi:10.1177/0954406216665416

Bond, W. L. (1948). A simple procedure for the making of alignment charts. *J. Appl. Phys.*, *19*(1), 83–86. doi:10.1063/1.1697877

Boulet, D., Doerfler, R., Marasco, J., & Roschier, L. (2020). *pyNomo documentation.* http://lefakkomies.github.io/pynomo-doc/index.html

de Freitas Avelar, A. H., Roschier, L., Fernandes Soares, L., & Oliveira Ávila, P. H. S. (2021). Analytical solutions and computational nomograms for maximum pressure angle for cam mechanisms for full and half cycloidal and harmonic motion curves. *J. Mech. Eng. Sci.*, *235*(15), 2725–2736. doi:10.1177/0954406220962823

d'Ocagne, M. (1899). *Traité de nomographie*. Paris: Gauthier-Villars.

Doerfler, R. (2009). On jargon — The lost art of nomography. *The UMAP Journal*, *30*(4), 457–493. https://www.comap.com/product/?idx=1048

Douglas, J., & Danciu, L. (2020). Nomogram to help explain probabilistic seismic hazard. *J. Seismol.*, *24*, 221–228. doi:10.1007/s10950-019-09885-4

Éidinov, M. S., Nyrko, V. A., Éidinov, R. M., & Gashukov, V. S. (1976). Torsional vibrations of a system with Hooke's joint. *Sov. Appl. Mech.*, *12*, 291–298. doi:10.1007/BF00884975

El-Shakery, S. A., & Terauchi, Y. (1984). A computer-aided method for optimum design of plate cam-size avoiding undercutting and separation phenomena—II: Design nomograms. *Mech. Mach. Theory*, *19*(2), 235–241. doi:10.1016/0094-114X(84)90046-6

Esmail, E. L. (2013). Nomographs for synthesis of epicyclic-type automatic transmissions. *Meccanica*, *48*, 2037–2049. doi:10.1007/s11012-013-9721-z

Esmail, E. L. (2016). Configuration design of ten-speed automatic transmissions with twelve-link three-DOF Lepelletier gear mechanism. *J. Mech. Sci. Technol.*, *30*, 211–220. doi:10.1007/s12206-015-1225-4

Esmail, E. L., & Hussen, H. A. (2010, November). Nomographs for kinematics, statics and power flow analysis of epicyclic gear trains. In *Proc. of the ASME 2009 Int. Mech. Eng. Congr. Expos.* (Vol. 13, pp. 631–640). Lake Buena Vista, USA: ASME. doi:10.1115/IMECE2009-10789

Esmail, E. L., Pennestrì, E., & Juber, A. H. (2018). Power losses in two-degrees-of-freedom planetary gear trains: a critical analysis of Radzimovsky's formulas. *Mech. Mach. Theory*, *128*, 191–204. doi:10.1016/j.mechmachtheory.2018.05.015

Evesham, H. A. (1986). Origins and development of nomography. *IEEE Ann. Hist. Comput.*, *8*(4), 324–333. doi:10.1109/MAHC.1986.10059

Evesham, H. A. (2010). *The history and development of nomography*. Docent Press. http://hdl.handle.net/10547/581287

Ferrara, G. E. (1940). Nomography for the electrical engineer. *Electr. Eng.*, *59*(12), 505–508. doi:10.1109/EE.1940.6435199

Gent, A. N. (1958). On the relation between indentation hardness and Young's modulus. *Rubber Chem. Technol.*, *31*(4), 896–906. doi:10.5254/1.3542351

Glasser, L., & Doerfler, R. (2019). A brief introduction to nomography: graphical representation of mathematical relationships. *Int. J. Math. Educ. Sci. Technol.*, *50*(8), 1273–1284. doi:10.1080/0020739X.2018.1527406

Grier, D. A. (2001). Human computers: the first pioneers of the information age. *Endeavour*, *25*(1), 28–32. doi:10.1016/S0160-9327(00)01338-7

Grimes, D. A. (2008). The nomogram epidemic: resurgence of a medical relic. *Ann. Intern. Med.*, *149*(4), 273–275. doi:10.7326/0003-4819-149-4-200808190-00010

Hain, K. (1961). Spring design and application. In N. P. Chironis (Ed.), (Vol. 276, pp. 274–275). McGraw-Hill, Inc.

Hankins, T. L. (1999). Blood, dirt, and nomograms: a particular history of graphs. *Isis*, *90*(1), 50–80. doi:10.1086/384241

Hassaan, G. A. (2015). Nomogram-based synthesis of complex planar mechanisms, part I: 6 bar-2 sliders mechanism. *Int. J. Eng. Techniques*, *1*(6), 29–35. https://scholar.cu.edu.eg/sites/default/files/galal/files/nomogram_pt_i.pdf

Hilbert, D. (1901). Mathematische probleme. *Archive für Mathematik und Physik*, *1*(1), 44–63.

Hilpert, H. (1968). Weight balancing of precision mechanical instruments. *Journal of Mechanisms*, *3*(4), 289–302. doi:10.1016/0022-2569(68)90005-0

Hohenberg, R. (1967). Detection and study of compressor-blade vibration. *Exp. Mech.*, *7*, 19A–24A. doi:10.1007/BF02327002

Howison, M. (2014). Constructing interactive nomograms. https://www.researchgate.net/profile/Mark-Howison/publication/228841217_Constructing_Interactive_Nomograms/links/0fcfd50f99431f12e8000000/Constructing-Interactive-Nomograms.pdf

Hwang, W.-M., & Chen, K.-H. (2007). Triangular nomograms for symmetrical spherical non-Grashof double-rockers generating symmetrical coupler curves. *Mech. Mach. Theory*, *42*(7), 871–888. doi:10.1016/j.mechmachtheory.2006.05.008

Kattan, M. W., & Marasco, J. (2010). What is a real nomogram? *Semin. Oncol.*, *37*(1), 23–26. doi:10.1053/j.seminoncol.2009.12.003

Khoshnevis, S., Brothers, R. M., & Diller, K. R. (2018). Level of cutaneous blood flow depression during cryotherapy depends on applied temperature: criteria for protocol design. *ASME J. of Medical Diagnostics*, *1*(4), 041007. doi:10.1115/1.4041463

Lu, D. M. (1999). A triangular nomogram for spherical symmetric coupler curves and its application to mechanism design. *J. Mech. Des.*, *121*(2), 323–326. doi:10.1115/1.2829463

Martínez-Pagán, P., & Roschier, L. (2022). Nomography: a renewed pedagogical tool to sciences and engineering high-education studies. *Heliyon*, *8*(6), e09731. doi:10.1016/j.heliyon.2022.e09731

Meyer zur Capellen, W. (1983). Nomogramme für die Krümmung sphärischer und ebener Bahnkurven. *Mech. Mach. Theory*, *18*(3), 249–254. doi:10.1016/0094-114X(83)90098-8

Miconi, D. (1987). Vibration control in industrial plant: a methodological approach. *J. Vib., Acoust., Stress, and Reliab.*, *109*(4), 335–342. doi:10.1115/1.3269450

Mottola, G., & Cocconcelli, M. (2022, April). Nomograms: an old tool with new applications. In M. Ceccarelli & R. López-García (Eds.), *Int. symp. on hist. of mach. and mech.* (pp. 314–329). Jaén, Spain: Springer. doi:10.1007/978-3-030-98499-1_26

Mottola, G., Cocconcelli, M., Rubini, R., & Carricato, M. (2022). Gravity compensation in robotics. In V. Arakelian (Ed.), (Vol. 115, pp. 229–273). Springer, Cham. doi:10.1007/978-3-030-95750-6_9

Radaelli, G., Gallego, J. A., & Herder, J. L. (2011). An energy approach to static balancing of systems with torsion stiffness. *J. Mech. Des.*, *133*(9), 091006. doi:10.1115/1.4004704

Seireg, A. A., & Houser, D. R. (1970). Evaluation of dynamic factors for spur and helical gears. *J. Eng. Ind.*, *92*(2), 504–514. doi:10.1115/1.3427790

Soreau, R. (1902). *Contributions à la théorie et aux applications de la nomographie*. Paris: Beranger. https://babel.hathitrust.org/cgi/pt?id=mdp.39015038775394

Tournès, D. (2000). Notes & debats — Pour une histoire du calcul graphique. *Rev. d'Histoire des Math.*, *6*(1), 127–161. http://www.numdam.org/item/RHM_2000__6_1_127_0/

Tournès, D. (2003). Du compas aux intégraphes: les instruments du calcul graphique. *Repères–IREM*, *50*, 63–84. https://publimath.univ-irem.fr/biblio/IWR03005.htm

Tournès, D. (2014). Mathematik und Anwendungen. In M. Foote, M. Schmitz, B. Skorsetz, & R. Tobies (Eds.), (pp. 26–32). ThILLM. https://hal.univ-reunion.fr/hal-01187206

Tournès, D. (2018). Let history into the mathematics classroom. In Évelyne Barbin et al. (Eds.), (pp. 101–114). Springer. doi:10.1007/978-3-319-57150-8_8

Warmus, M. (1959). *Nomographic functions*. Warsaw: Państwowe Wydawnictwo Naukowe.

Wellauer, E. J., & Holloway, G. A. (1976). Application of EHD oil film theory to industrial gear drives. *J. Eng. Ind.*, *98*(2), 626–631. doi:10.1115/1.3438951

Wunderlich, W. (1980). Nomogramme für die Wattsche Geradführung. *Mech. Mach. Theory*, *15*(1), 5–8. doi:10.1016/0094-114X(80)90028-2

Young, W. C., & Budynas, R. G. (2002). *Roark's formulas for stress and strain*. McGraw-Hill.

Zotov, N. M., & Balakina, E. V. (2007). Using the $\varphi - s_x$ nomogram in calculating the dynamics of a braked wheel. *J. Mach. Manuf. Reliab.*, *36*, 193–198. doi:10.3103/S1052618807020161

Vitae

Giovanni Mottola was born in Italy on August 10, 1990. He received the M.S. degree in mechanical engineering and the Ph.D. degree in applied mechanics from the University of Bologna, Bologna, Italy, in 2015 and 2019, respectively. In 2017, he has been a visiting researcher at the Laval Robotics Laboratory at Université Laval (Québec, Canada). In 2020, he joined the University of Modena and Reggio Emilia, Reggio Emilia, Italy, where he is currently a Contract Researcher in applied mechanics in the Department of Sciences and Methods of Engineering. His research interests include parallel robots, machine diagnostics, and history of mechanical engineering.

Marco Cocconcelli was born in Italy on November 9, 1977. He received the M.S. degree in mechanical engineering and the Ph.D. degree in applied mechanics from the University of Bologna, Bologna, Italy, in 2003 and 2007, respectively. In 2007, he joined the University of Modena and Reggio Emilia, Reggio Emilia, Italy, where he is currently an associate professor in Applied Mechanics at the Department of Sciences and Methods for Engineering. His research interests include diagnostics of bearings and gears, condition monitoring of machinery, and history of mechanisms and machine science. He is a member of the Italian branch of the International Federation for the Promotion of Mechanism and Machine Science (IFToMM-Italy).